

Hovering Control of a Quadrotor UAV

Angel Flores-Abad¹, Manuel Nandayapa² and Antonio Flores Camacho³

Abstract—Quadrotors have attracted the attention of the academia, companies and hobbyists for the last decade. One of the main advantages of the Quadrotors is the capability to perform vertical take-off and landing, which makes possible a quick autonomous hover. In this paper, the development of a hovering control for a Quadrotor UAV using typical control techniques is presented. The Quadrotor is equipped with an onboard IMU which provides linear acceleration and angular velocity measurements. The Euler angles that represent the attitude of the system are estimated using the rate gyro's measurements and some kinematics relations. A hobby Quadrotor with an Ardupilot 2.6 is used as test bed. A simulation study and real-time implementation in indoor and outdoor environments demonstrate the effectiveness of the proposed control scheme.

I. INTRODUCTION

A major drawback of helicopters-like unmanned aerial vehicles (UAVs) is the need of extensive and costly maintenance for reliable operation. Simplification of the mechanical structure produces several benefits [1]. Quadrotors are an alternative type of UAVs that do not include the complicated swash plates and linkages found in conventional designs and instead use variation in its four rotors speed to maneuver. Due to the reduction in the mechanical and control complexity, Quadrotors are being proposed in several applications, such as: surveillance, traffic monitoring, agriculture, search and rescue, and so on. Currently, many UAV researchers are using this type of vehicle as their platforms to study: UAV dynamics [2], [3], autonomous control techniques [4], [5], multi-vehicle cooperative manipulation motion planning [6], state estimation [7] and perception [8], [9]. However, some of those works have been tested under very ideal indoor conditions where the air forces are negligible, such a scenario is unrealistic, because the dynamics of Quadrotors highly sensitive to air conditions. Besides, in those works, the algorithms rely on measurements obtained from a motion capture system, which is impossible to have in a real situation.

In this work we present a hovering control for a Quadrotor that is tested in a realistic environment with difficult air conditions. In order to achieve such a goal, we designed two PD controllers, one for the attitude and the other for the altitude. The designed algorithms are first implemented in a open source Quadrotor simulator to gain some insight in the performance of the system and to obtain a first try for the controllers' gains. Later, an Ardupilot 2.6 platform of 3D robotics is employed as the measuring and control platform.

A Quadrotor is a rotatory-wing craft that has four motors located in the front, rear, left and right ends of a cross-frame. The Quadrotor maneuvers are controlled by changing the rotating speed of each motor. As shown in Figure 1, rotors 1 and 3 rotate clockwise and rotors 2 and 4 rotate counter-clockwise. As a result, it is possible to balance the total torque created. The relative speed between the left and right rotors is varied to control the roll rate of the UAV. A Quadrotor hovers or adjusts its altitude by applying equal thrusts to all four rotors. The pitch rate is controlled by applying more thrust to rotors rotating in one direction, e.g. rotors 1 and 3. A Quadrotor adjusts its pitch or roll by applying more thrust to its diametrically rotor.

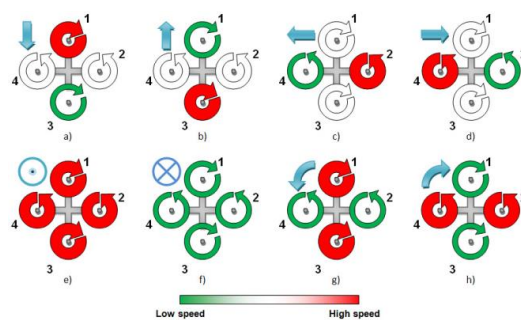


Fig. 1. Different Quadrotor maneuvers depending on the speed and direction of the blades rotation.

The rest of the paper is organized as follows, section II describes the Quadrotor used in this work for experimental validation. Section III presents the kinematics and dynamics modelling of the vehicle. Section IV introduces the controller design to achieve autonomous hovering. Section V is devoted to a simulation analysis of the system. Section VI provides the results obtained from indoor and outdoor real time experiments. Finally, section VII concludes the paper.

II. QUADROTOR PLATFORM

A picture of our aerial platform, the Storm Drone 4, is depicted in Figure 2 and its main specifications are listed in Table I. In order to perform autonomous hovering control we use ardupilot 2.6 which includes a 3-axis gyro and 3-axis accelerometer; a 4 MegaByte Dataflash chip for automatic datalogging; a barometric pressure; a GPS; a compass; telemetry devices; and Atmel's ATMEGA2560 and ATMEGA32U-2 chips for processing and usb functions, respectively.

¹Angel Flores-Abad is with Autonomous University of Ciudad Juarez, Ciudad Juarez, Ch. 32310, Mexico anflores@uacj.mx

²Manuel Nandayapa is with Autonomous University of Ciudad Juarez, Ciudad Juarez, Ch. 32310, Mexico, mnandaya@uacj.mx

³Antonio Flores Camacho is with Autonomous University of Ciudad Juarez, Ciudad Juarez, Ch. 32310, Mexico, tonyfcl9@gmail.com



Fig. 2. The Quadrotor Storm Drone 4 and an Ardupilot onboard.

TABLE I
 SPECIFICATIONS OF THE QUADROTOR STORM DRONE 4.

Components	Value/Quantity
Propellers	8 in / 4
Weight	400 gr
Battery	3S Lipo / 1
Electronic Speed Controller (ESC)	10A / 4
Motors	400W-kv 1050 / 4
Payload	400 gr

III. MODELLING

A. Kinematics

To derive the kinematics model of the Quadrotor, let's define two coordinate systems, as shown in Figure 3. One is the world reference frame $\mathcal{W} = \{^W X, ^W Y, ^W Z\}$ fixed to ground with its $^W Z$ axis pointing vertically downward in the gravity direction. The other is the body frame $\mathcal{B} = \{^B X, ^B Y, ^B Z\}$ attached to the center of mass (CM) of the Quadrotor, where the $^B Z$ axis is assumed perpendicular to the face of the Quadrotor and pointing against the thrust direction and the $^B X$ axis is coinciding with the forward direction and aligns with rotor 1. Finally the $^B Y$ axis is allocated using the right-hand-rule. Using the Z-X-Y, the Quadrotor orientation in the world frame is given by the rotation matrix $\mathbf{R} \in \mathbb{R}^{3 \times 3} : \mathcal{B} \rightarrow \mathcal{W}$ as

$$\mathbf{R} = \begin{bmatrix} c_\beta c_\alpha & -c_\beta s_\alpha & s_\beta \\ c_\alpha s_\gamma - c_\gamma s_\alpha s_\beta & c_\alpha s_\gamma + s_\alpha s_\beta s_\gamma & c_\beta s_\alpha \\ s_\alpha s_\gamma + c_\alpha c_\gamma s_\beta & c_\gamma s_\alpha - c_\alpha c_\gamma s_\beta & -c_\alpha c_\gamma \end{bmatrix} \quad (1)$$

where α, β and γ are the roll, pitch and yaw angles, respectively, besides $c = \cos(\cdot)$ and $s = \sin(\cdot)$.

Let the vector $\boldsymbol{\omega} = [\omega_x \ \omega_y \ \omega_z]^T$ represent the angular velocity in frame \mathcal{B} , which is measured by the IMU through onboard gyro sensors and $\boldsymbol{\theta} = [\alpha \ \beta \ \gamma]^T$ the Euler angles vector. Then ${}^B \boldsymbol{\omega}$ is related to the time rates of the three Euler angles by

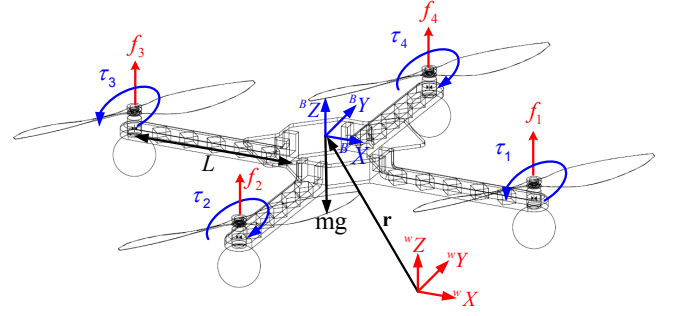


Fig. 3. Free body diagram showing the inertial and body frames.

$$\boldsymbol{\omega} = \begin{bmatrix} \omega_x \\ \omega_y \\ \omega_z \end{bmatrix} = \begin{bmatrix} c\theta & 0 & -c\phi s\theta \\ 0 & 1 & s\phi \\ 0 & s\theta & c\phi c\theta \end{bmatrix} \begin{bmatrix} \dot{\phi} \\ \dot{\theta} \\ \dot{\psi} \end{bmatrix} = \mathbf{H}\dot{\boldsymbol{\theta}} \quad (2)$$

Then, solving for the time derivative of the Euler angles we get

$$\dot{\boldsymbol{\theta}} = \mathbf{H}^{-1}\boldsymbol{\omega} = \begin{bmatrix} 0 & s_\alpha t_\beta & -c_\alpha t_\beta \\ 0 & c_\alpha & s_\alpha \\ 1 & s_\alpha/c_\beta & c_\alpha/c_\beta \end{bmatrix} \begin{bmatrix} \omega_x \\ \omega_y \\ \omega_z \end{bmatrix} \quad (3)$$

Since, (3) is nonlinear, by numerical integrating the Euler angles vector $\boldsymbol{\theta}$ is obtained.

B. Dynamics

As shown in Figure 3, during a hovering maneuver, the whole system will be subjected to the force due to the mass of the Quadrotor m , the gravity force i.e. mg and the lifting forces $f_i (i = 1, 2, 3, 4)$ which are produced by the four rotors. By Newton-Euler formulation, we get the following equations of motion:

$$m_Q \ddot{\mathbf{r}} = \begin{bmatrix} 0 \\ 0 \\ m_Q g \end{bmatrix} + \mathbf{R} \begin{bmatrix} 0 \\ 0 \\ T \end{bmatrix} \quad (4)$$

where $T = f_1 + f_2 + f_3 + f_4$ is the total thrust provided by the four motors. Besides

$$\boldsymbol{\tau} = \mathbf{I}\dot{\boldsymbol{\omega}} + \boldsymbol{\omega} \times \mathbf{I}\boldsymbol{\omega} \quad (5)$$

where $\boldsymbol{\tau} \in \mathbb{R}^3$ is the resultant torque applied to the UAV system, $\mathbf{I} \in \mathbb{R}^{3 \times 3}$ is the inertial tensor of the system; $\boldsymbol{\omega} \in \mathbb{R}^3$ is the angular velocity of the system; $\dot{\boldsymbol{\omega}} \in \mathbb{R}^3$ is the angular acceleration. For convenience, all of these variables are represented in the body fixed frame. Equation 5 can be written in detail as

$$\mathbf{I} \begin{bmatrix} \dot{\omega}_x \\ \dot{\omega}_y \\ \dot{\omega}_z \end{bmatrix} = \begin{bmatrix} L(f_4 - f_2) \\ L(f_1 - f_3) \\ \tau_2 + \tau_4 - \tau_1 - \tau_3 \end{bmatrix} - \begin{bmatrix} \omega_x \\ \omega_y \\ \omega_z \end{bmatrix} \times \mathbf{I} \begin{bmatrix} \omega_x \\ \omega_y \\ \omega_z \end{bmatrix} \quad (6)$$

where L is the distance from each rotor to the Quadrotor's CM.

C. Propulsion Model

The Quadrotor uses four DC brushless motors for propulsion and control. For dynamics modeling, we need to know the lift force f_i and torque τ_i in terms of the rotating speed of each rotor, ω_i . The steady-state thrust force generated by a rotor in air can be modeled as [6]

$$f_i = C_T \rho A_r r^2 \omega_i^2 \quad (7)$$

where A_r is the rotor disk area; r is the radius; ω_i is the rotor speed; C_T is the thrust coefficient that depends on rotor geometry and profile; and ρ is the density of air. In practice, the lift force model can be simplified as

$$f_i = k_f \omega_i^2 \quad (8)$$

where k_f is the lift force constant. Besides, the rotating rotors will also produce torques τ_i ($i = 1, 2, 3, 4$) which are perpendicular to the face of the Quadrotor, given by

$$\tau_i = k_\tau \omega_i^2 \quad (9)$$

where k_τ is the torque constant.

IV. CONTROL SYSTEM SCHEME

In order to achieve autonomous hovering both attitude and altitude must be controlled. As mentioned in the introduction, several control algorithms have been implemented on the Quadrotors for this purpose. Nevertheless, in practice, the performance of a conventional control of the PID's family is competitive with most of advanced controllers. Figure 4 shows a block diagram of our control scheme.

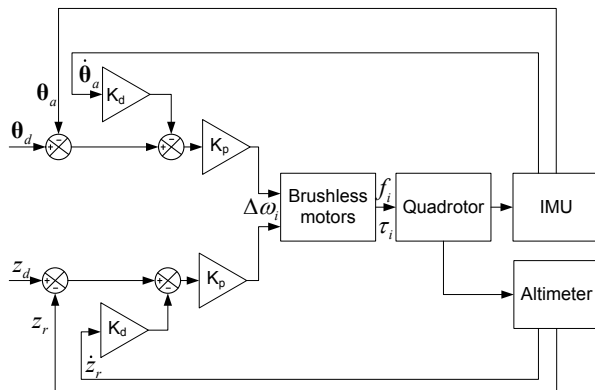


Fig. 4. Control scheme block diagram.

One can observe in Figure 4 that outputs of the controllers are not the torques that the motors should produce, but its rotational speed. By controlling the speed of the four rotors, specific thrusts and torques are generated so that the desired attitude and altitude values are attained.

V. SIMULATION STUDY

With the purpose of studying the dynamics and behavior of a Quadrotor, as a first step, we used the open source simulator provide by P. Corke [10], where we implemented the control algorithm depicted in Figure 4. Since, our objective is to achieve autonomous hovering control, our desired values are $\theta_d = [\alpha_d \ \beta_d \ \gamma_d]^T = [0 \ 0 \ 0 \ t]^T$ rad and the desired altitude is $r_d(3) = z_d = 4$ m. We selected Kp and Kd to be 2.5 and -100, respectively. As can be observed in Figure 5, the three Euler angles are very close to zero, and in Figure 6 the altitude after a few seconds and a small overshoot rise to the desired value, i.e. 4 m in the vertical positive direction. Besides, Figure 7 shows the final result of the animation included in the simulator, where one can observe that effectively, the three orientation angles of the vehicle are zero and that the Quadrotor flow to an altitude of 4 m.

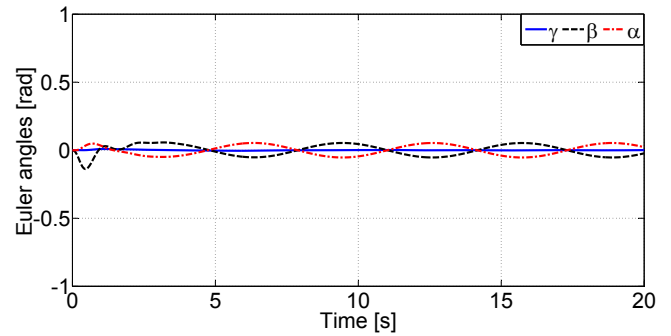


Fig. 5. Euler angles resulting from the implementation of the proposed control scheme in a simulator.

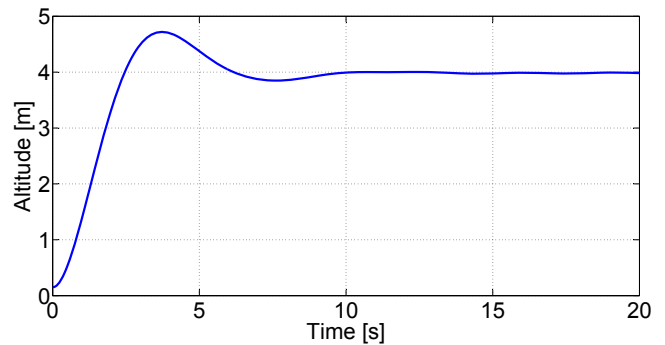


Fig. 6. Quadrotor's Altitude during the simulation study.

VI. REAL TIME IMPLEMENTATION

Figure 8 illustrate the main components of the real system. It is important to mention that the Electronic Speed Controllers (ESC) should receive a PWM signal with a frequency of 50 Hz and a duty cycle of 5-10%.

A. Indoor Test

One must be very careful and take safety measures when working with Quadrotors, as the propellers are rotating to very high speed and any contact with them may hurt the user.

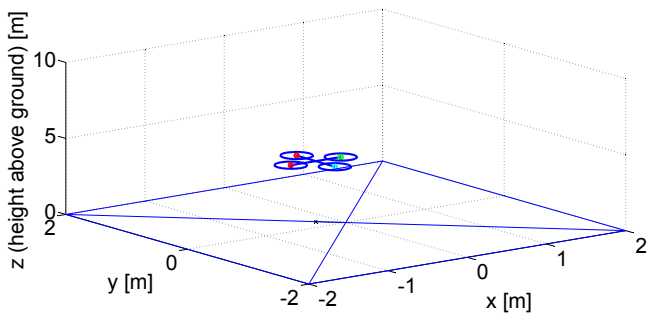


Fig. 7. Snapshot of the inflight animation.

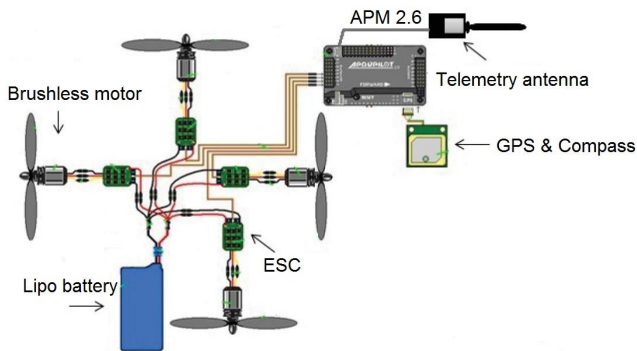


Fig. 8. Electrical connections of the system.

Plus, RC communication can be lost and then the vehicle goes out of control. Because of those conditions, before proceeding to perform outdoor tests, we executed several indoor and constrained tests. Figure 9 is a picture of the Quadrotor hovering autonomously inside a room constrained with a couple of cords to avoid any collision risk in case something goes abnormal. In this case, the desired values for the roll and pitch angle are set equal to zero rad and the yaw angle to -1.4 rad. Figures 10, 11 and 12 depict the pitch, roll and yaw angles for this particular test. It is observed that, in all three cases, the deviations from the set point are very small, in the order of a few tenths of radians.



Fig. 9. Quadrotor hovering autonomously in a constrained indoor experiment.

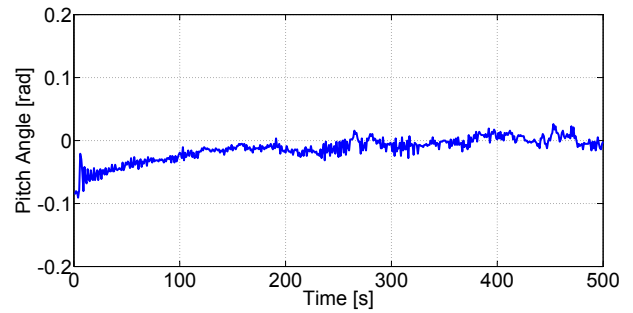


Fig. 10. Pitch angle during the indoor test.

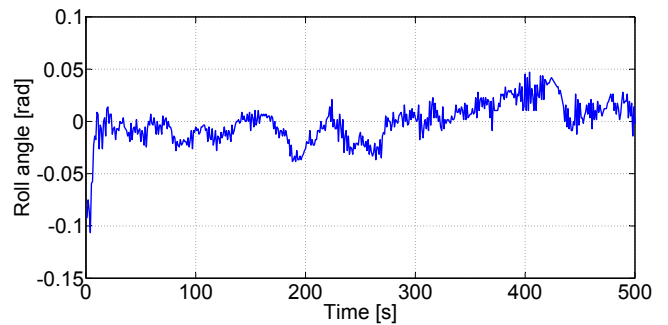


Fig. 11. Roll angle during the indoor test.

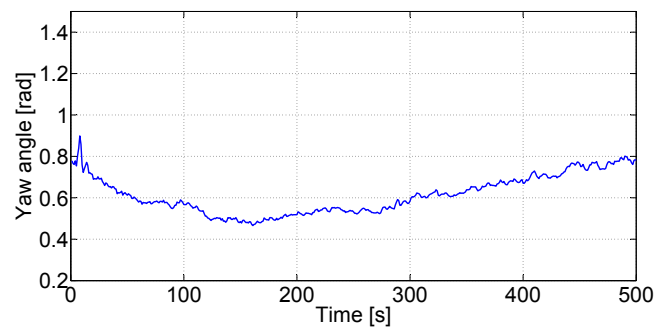


Fig. 12. Yaw angle during the indoor test.

B. Outdoor Test

An outdoor test was designed and conducted to verify the performance of our control system in a real situation with the inconvenience of the air disturbances. In this scenario, we left the Quadrotor to fly freely in accordance with the control commands. In Figure 13, we can see the vehicle hovering to a predefined altitude given by an open-loop command. Despite of the presence of some airstreams, the orientation of the aircraft still remained bounded very close to the desired value (as observed in Figures 14, 15 and 16). In this test, the actual values are a little bit more deviated from the desired value than those in the indoor case, which is understandable because of the environment conditions. Nevertheless, the actual values are still very close to the set point.



Fig. 13. Quadrotor hovering autonomously in an outdoor test.

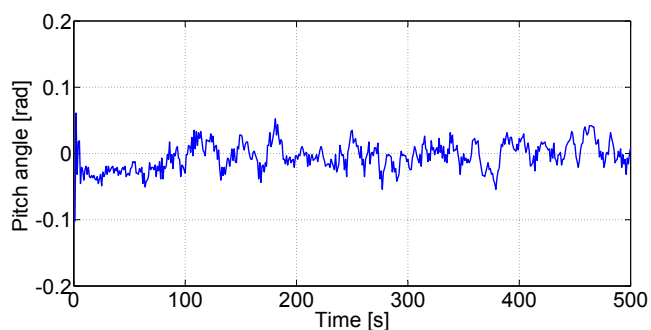


Fig. 14. Pitch angle during a outdoor test with difficult air conditions.

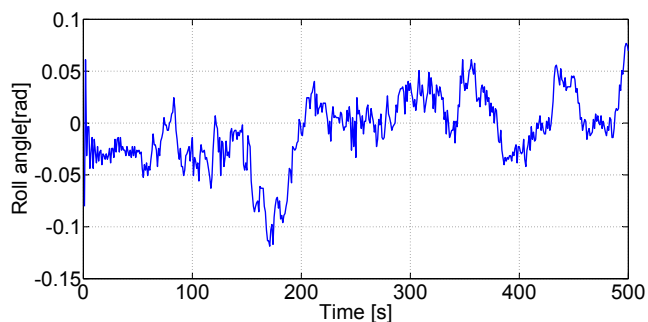


Fig. 15. Roll angle during a outdoor test with difficult air conditions.

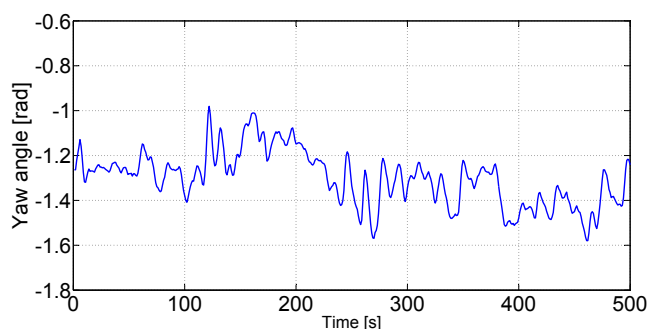


Fig. 16. Yaw angle during a outdoor test with difficult air conditions.

VII. CONCLUSIONS

The design, simulation and implementation of an autonomous hovering controller for a Quadrotor aircraft was presented. A hobbyist vehicle Storm Drone 4 and an Ardupilot 2.6 are the main components of our test platform. The simulation study provided a prudent first step to get familiar with the dynamics of the Quadrotor. The implemented control algorithm corresponds to a typical PID scheme, which demonstrated to be capable of achieving hovering control not only in indoor but also in outdoor conditions, where the air disturbs the vehicle significantly. In the future, a position and trajectory tracking controllers will be implemented, as well as a more advanced attitude control.

REFERENCES

- [1] P. Pounds, R. Mahony, and P. Corke, "Modelling and control of a large quadrotor robot," *Control Engineering Practice*, vol. 18, no. 7, pp. 691–699, 2010.
- [2] G. M. Hoffmann, H. Huang, S. L. Waslander, and C. J. Tomlin, "Quadrotor helicopter flight dynamics and control: Theory and experiment," in *AIAA Guidance, Navigation, and Control Conference*, South Carolina, 2007.
- [3] L. R. G. Carrillo, A. E. D. López, R. Lozano, and C. Pégard, "Modeling the quad-rotor mini-rotorcraft," in *Quad Rotorcraft Control*. Springer, 2013, pp. 23–34.
- [4] S. Bouabdallah and R. Siegwart, "Backstepping and sliding-mode techniques applied to an indoor micro quadrotor," in *IEEE International Conference on Robotics and Automation*, Barcelona, Spain.
- [5] O. Purwin and R. D'Andrea, "Performing aggressive maneuvers using iterative learning control," in *IEEE International Conference on Robotics and Automation*, Kobe, Japan, 2009, pp. 1731–1736.
- [6] N. Michael, D. Mellinger, Q. Lindsey, and V. Kumar, "The grasp multiple micro-uav testbed," *IEEE Robotics & Automation Magazine*, vol. 17, no. 3, pp. 56–65, 2010.
- [7] N. Abas, A. Legowo, and R. Akmeliawati, "Parameter identification of an autonomous quadrotor," in *International Conference On Mechatronics*, Kuala Lumpur, 2011, pp. 1–8.
- [8] C. S. Sharp, O. Shakernia, and S. S. Sastry, "A vision system for landing an unmanned aerial vehicle," in *IEEE International Conference on Robotics and Automation*, Seoul, Korea, 2001, pp. 1720–1727.
- [9] S. Scherer, S. Singh, L. Chamberlain, and S. Saripalli, "Flying fast and low among obstacles," in *IEEE International Conference on Robotics and Automation*, Roma, Italy.
- [10] P. Corke, "A robotics toolbox for matlab," *IEEE Robotics & Automation Magazine*, vol. 3, no. 1, pp. 24–32, 1996.